VIROLOGY

# Durable sequence stability and bone marrow tropism in a macaque model of human pegivirus infection

Adam L. Bailey,[1,2] Michael Lauck,[1,2] Mariel Mohns,[1,2] Eric J. Peterson,[2] Kerry Beheler,[2] Kevin G. Brunner,[2] Kristin Crosno,[2] Andres Mejia,[2] James Mutschler,[2,3] Matthew Gehrke,[1,2] Justin Greene,[1,2] Adam J. Ericsen,[1,2] Andrea Weiler,[2,3] Gabrielle Lehrer-Brey,[2,3] Thomas C. Friedrich,[2,3] Samuel D. Sibley,[2,3] Esper G. Kallas,[4] Saverio Capuano III,[2] Jeffrey Rogers,[2,5] Tony L. Goldberg,[2,3] Heather A. Simmons,[2] David H. O'Connor[1,2]*

**Human pegivirus (HPgV)—formerly known as GB virus C and hepatitis G virus—is a poorly characterized RNA virus that infects about one-sixth of the global human population and is transmitted frequently in the blood supply. We create an animal model of HPgV infection by infecting macaque monkeys with a new simian pegivirus (SPgV) discovered in wild baboons. Using this model, we provide a high-resolution, longitudinal picture of SPgV viremia where the dose, route, and timing of infection are known. We detail the highly variable acute phase of SPgV infection, showing that the viral load trajectory early in infection is dependent on the infecting dose, whereas the chronic-phase viremic set point is not. We also show that SPgV has an extremely low propensity for accumulating sequence variation, with no consensus-level variants detected during the acute phase of infection and an average of only 1.5 variants generated per 100 infection-days. Finally, we show that SPgV RNA is highly concentrated in only two tissues: spleen and bone marrow, with bone marrow likely producing most of the virus detected in plasma. Together, these results reconcile several paradoxical observations from cross-sectional analyses of HPgV in humans and provide an animal model for studying pegivirus biology.**

## INTRODUCTION

Few RNA viruses sustain high-titer viremia in humans. Those that do have evolved extensive mechanisms to evade host immune responses and induce pathological inflammation and disease over time. Human pegivirus (HPgV)—formerly known as GB virus C (GBV-C) and also as hepatitis G virus (HGV)—infects about one-sixth of the global human population and is transmitted frequently in the blood supply of the United States, yet little is known about the biology of this virus (*1*). HPgV belongs to the newly formed *Pegivirus* genus within the Flaviviridae family of positive-sense, single-stranded RNA viruses (*2*). Persistent, high-titer viremia is a hallmark of HPgV infection, but infection appears to be benign: it is asymptomatic and causes no overt pathology (*3*, *4*).

Several epidemiological studies suggest that HPgV co-infection may be beneficial in the context of other viral infections that induce immune-mediated pathology (*5*–*7*). In particular, HIV-infected individuals co-infected with HPgV are protected from HIV-associated immune activation (*8*) and experience a 2.5-fold reduction in all-cause mortality compared to those infected with HIV only [see (*9*) for a meta-analysis and (*1*) for a review]. Although many plausible mechanisms as to how HPgV may mediate this protective effect have been proposed, compelling in vivo data in support of a unifying mechanism are still lacking. Cross-sectional studies suggest that HPgV infection varies considerably between individuals and that HPgV may replicate within tissues that are difficult to access (for example, spleen and bone marrow). Furthermore, no animal model of HPgV infection currently exists. A macaque monkey (*Macaca* spp.) model of HPgV infection has long been sought, in part because the infection of macaques with simian immunodeficiency virus (SIV) is the most well-studied and established animal model of HIV infection (*10*). However, despite two reports documenting the infection of macaques with HPgV in the early 2000s (*11*, *12*), several recent efforts to infect macaques with HPgV have been unsuccessful (J. Stapleton, personal communication). HPgV can persistently infect chimpanzees (*Pan troglodytes*) (*13*), but the use of chimpanzees in biomedical research has recently been reevaluated and is no longer ethically justifiable (*14*).

We recently described the first pegiviruses infecting Old World (that is, *cercopithecoid*) monkeys (*15*). These simian pegiviruses (SPgVs) were identified in red colobus monkeys (*Procolobus tephrosceles*; SPgVkrc), red-tailed guenons (*Cercopithecus ascanius*; SPgVkrtg), and an olive baboon (*Papio anubis*; SPgVkob) living in Kibale National Park, Uganda, and formed a distinct clade with respect to the Great Ape and New World monkey SPgVs. Here, we extend the geographic and host range of the Old World monkey SPgVs with the discovery of a new SPgV in samples collected from yellow baboons (*Papio cynocephalus*; SPgVmyb) in Mikumi National Park, Tanzania, and use baboon SPgVs to create a macaque model of HPgV infection.

## RESULTS

### Baboons naturally harbor distinct pegiviruses

As part of our ongoing effort to discover new viruses in wild nonhuman primates, we applied unbiased deep sequencing to plasma samples collected from 43 wild yellow baboons living in Mikumi National Park, Tanzania, during 1985 and 1986. In 17 of these animals (40%), we detected a new SPgV (SPgVmyb) and were able to assemble 14 coding-complete SPgVmyb genomes (Fig. 1A and table S1). In a phylogenetic analysis, these viruses grouped with other Old World monkey SPgVs

[1]Department of Pathology and Laboratory Medicine, University of Wisconsin–Madison, Madison, WI 53711, USA. [2]Wisconsin National Primate Research Center, Madison, WI 53711, USA. [3]Department of Pathobiological Sciences, University of Wisconsin–Madison, Madison, WI 53711, USA. [4]Division of Clinical Immunology and Allergy, School of Medicine, University of São Paulo, São Paulo 01310-911, Brazil. [5]Human Genome Sequencing Center, Baylor College of Medicine, Houston, TX 77030, USA.
*Corresponding author. E-mail: doconnor@primate.wisc.edu

and were most closely related to SPgVkob (Fig. 1B). However, plasma viral loads obtained by quantitative reverse transcription polymerase chain reaction (RT-qPCR) for SPgVmyb-infected yellow baboons (average, $2.7 \times 10^5 \pm 7.3 \times 10^4$, SEM) were significantly less than the plasma viral load observed for the single SPgVkob-infected olive baboon identified previously ($2.4 \times 10^7$) (Fig. 2, A and B) (*15*).

## Baboon SPgVs infect macaques

Among the monkey species in which we have discovered SPgVs, baboons are most closely related to macaques (Fig. 1C). Therefore, in an attempt to create an in vivo laboratory model of HPgV infection, we inoculated a Mauritian-origin cynomolgus macaque (cy0571) intravenously with 0.5 ml of plasma pooled from two Mikumi yellow baboons

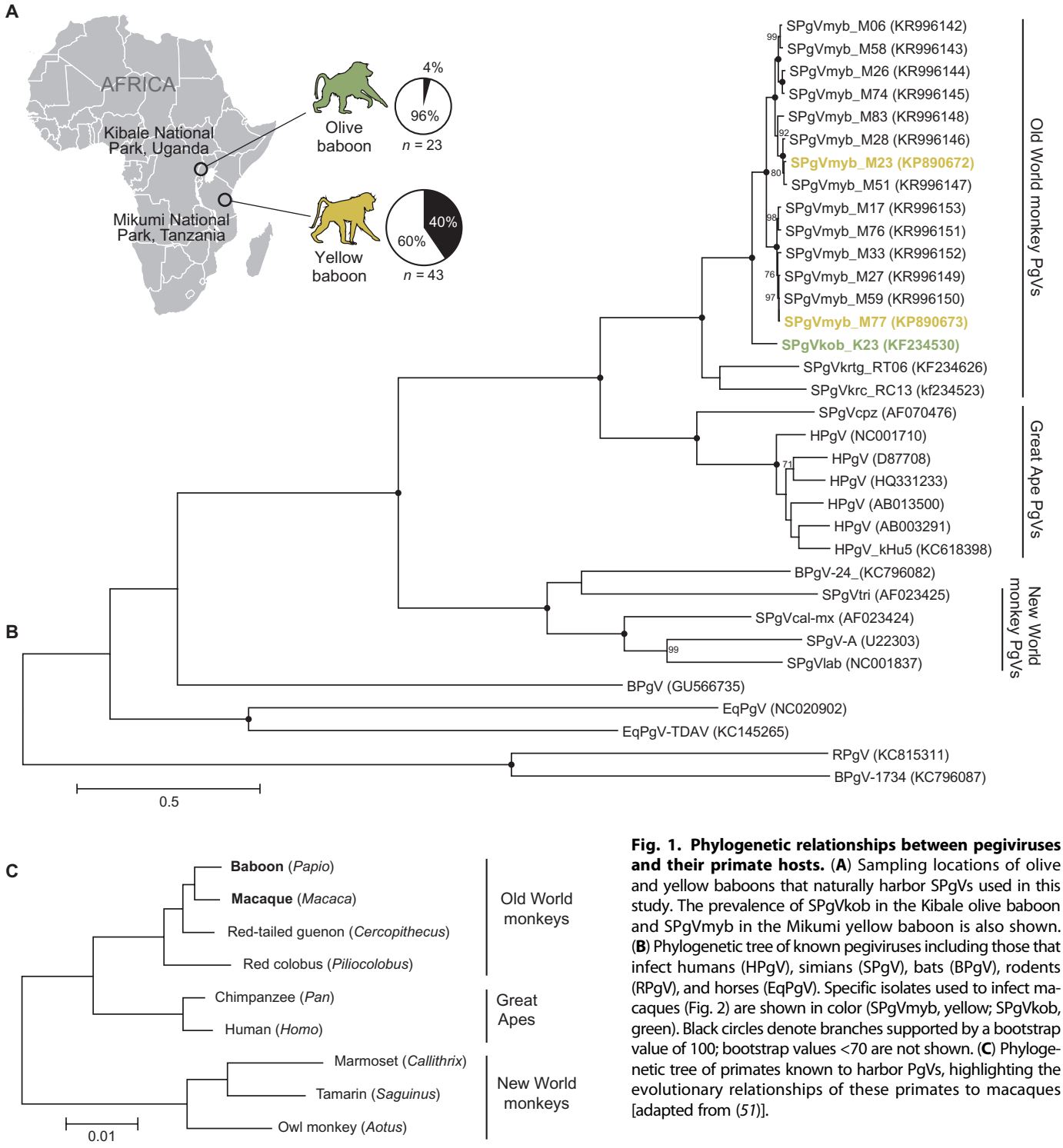


**Fig. 1. Phylogenetic relationships between pegiviruses and their primate hosts.** (**A**) Sampling locations of olive and yellow baboons that naturally harbor SPgVs used in this study. The prevalence of SPgVkob in the Kibale olive baboon and SPgVmyb in the Mikumi yellow baboon is also shown. (**B**) Phylogenetic tree of known pegiviruses including those that infect humans (HPgV), simians (SPgV), bats (BPgV), rodents (RPgV), and horses (EqPgV). Specific isolates used to infect macaques (Fig. 2) are shown in color (SPgVmyb, yellow; SPgVkob, green). Black circles denote branches supported by a bootstrap value of 100; bootstrap values <70 are not shown. (**C**) Phylogenetic tree of primates known to harbor PgVs, highlighting the evolutionary relationships of these primates to macaques [adapted from (*51*)].

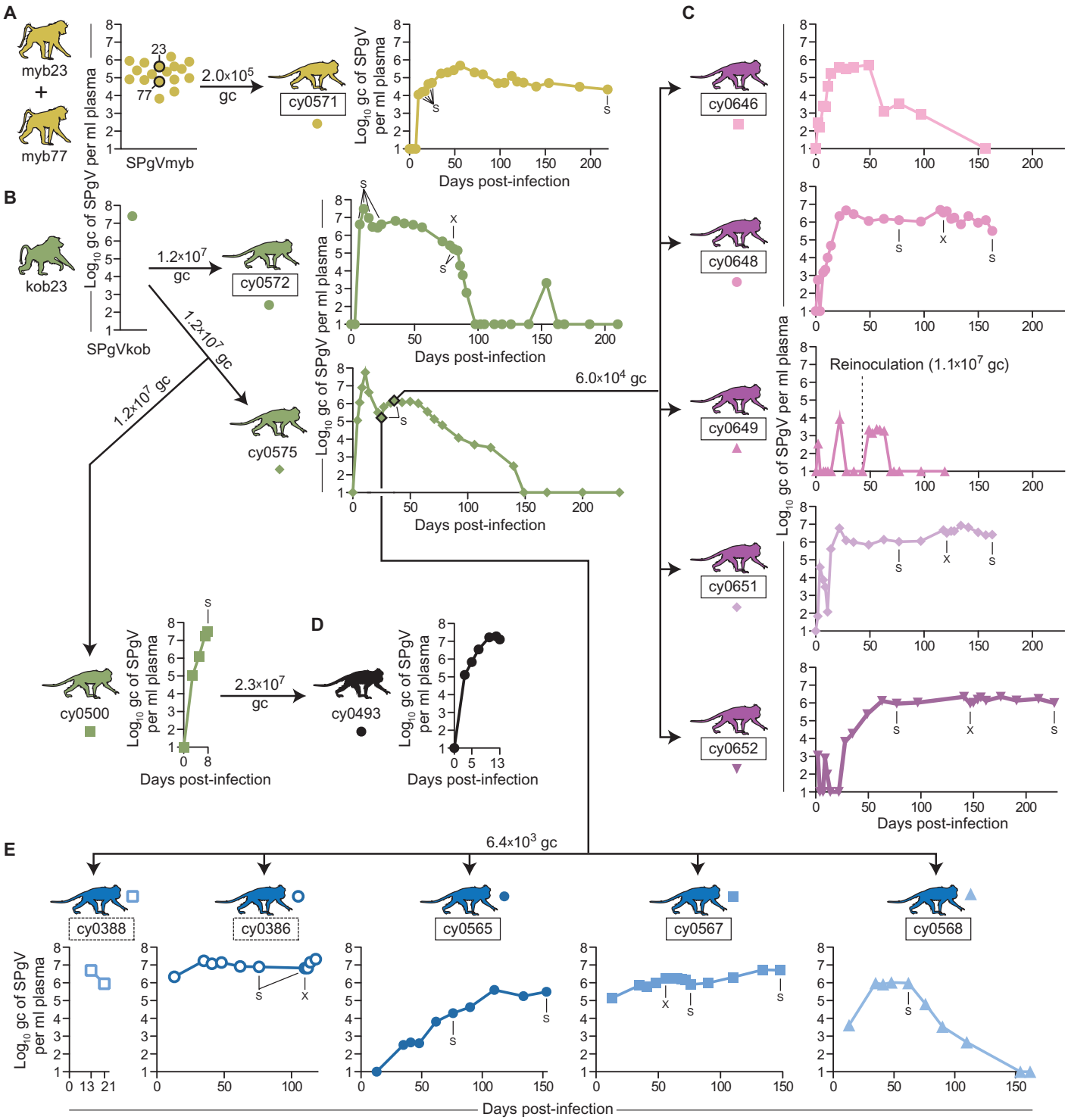


**Fig. 2. Infection of macaques with baboon SPgVs.** (**A**) Plasma SPgVmyb viral loads in the Mikumi yellow baboons (yellow) and the longitudinal viral loads from cy0571 infected with SPgVmyb. (**B** to **E**) Plasma SPgVkob viral load in the single Kibale olive baboon (green) and the longitudinal viral loads of macaques infected with SPgVkob from olive baboon plasma (green), cy0500 plasma collected at 8 dpi (D, black), or cy0575 plasma collected at 25 dpi (E, blue, male) or 36 dpi (C, pink, female). *Y* axis, $\log_{10}$ SPgV gc per milliliter of plasma; *x* axis, days post-infection unless otherwise stated. Specific colors and symbols refer to the same animal throughout the manuscript. Animal IDs surrounded by a box indicate SIVmac239 infection before SPgV inoculation, with dashed boxes signifying SIVmac239Δnef infection/vaccination. Additional information about each animal can be found in table S2. S, whole genome sequencing; X, splenectomy.

(baboons M23 and M77) containing a total of $2.0 \times 10^5$ genome copies (gc) of SPgVmyb (Fig. 2A). A second macaque (cy0572) was inoculated intravenously with 0.5 ml of Kibale olive baboon plasma (baboon K23) containing $1.2 \times 10^7$ gc of SPgVkob (Fig. 2B). Before inoculation of these macaques, baboon plasma samples were screened for additional microbes (for example, simian arteriviruses) using a combination of unbiased deep sequencing, RT-PCR, RT-qPCR, and culture-based techniques (*16*–*18*). Blood was drawn from each macaque and assayed biweekly for the presence of SPgV using RT-qPCR assays specific for each virus.

SPgVmyb was first detected in the plasma of cy0571 at $1.1 \times 10^4$ gc/ml 10 days post-inoculation (dpi) and slowly increased to a peak of $4.8 \times 10^5$ gc/ml at 56 dpi before gradually declining to a "set point" of $3.0 \times 10^4$ gc/ml, which was maintained until the animal was euthanized at 219 dpi (Fig. 2A). (Set point was defined throughout this study as the average of at least three viral load measurements, taken over a period of at least 25 days, that did not differ by more than 1 $\log_{10}$.) In contrast, SPgVkob was first detected in the plasma of cy0572 at $4.1 \times 10^6$ gc/ml 7 dpi and rapidly increased to a peak of $3.1 \times 10^7$ gc/ml by 10 dpi (Fig. 2B). By 21 dpi, viremia had reached a relative nadir of $2.7 \times 10^6$ gc/ml but then gradually increased to a set point of $4.5 \times 10^6$ gc/ml, which was maintained for 31 days before rapidly declining to undetectable by 98 dpi.

### Infecting dose dictates acute-phase SPgV viral load trajectory but not chronic-phase viremic set point

To examine viremia in a larger number of individuals, two additional cynomolgus macaques (cy0575 and cy0500) were infected with olive baboon plasma containing SPgVkob as done previously (Fig. 2B), and plasma from these animals was passaged into 11 additional cynomolgus macaques (Fig. 2, C to E). These macaques were repurposed from several other infection studies, and several were SIV-positive. However, heterogeneity in the infecting strain of SIV, the duration of SIV infection, and host genetic factors precluded us from examining the effect of SPgV co-infection on SIV pathogenesis (table S2 and fig. S1). We found that the acute phase of SPgV viremia was highly dependent on the infecting dose, with high-dose infections ($1.2 \times 10^7$ gc to $2.3 \times 10^7$ gc) reproducibly achieving a high-titer peak of viremia within the first 8 to 12 dpi, whereas low-dose infections ($6.4 \times 10^3$ gc to $6.0 \times 10^4$ gc) had a highly variable acute-phase viral load trajectory, with several animals not reaching their lifetime maximum of viremia until after 100 dpi (Fig. 3, A to C). Longitudinal viral load analysis in SPgVkob-infected macaques revealed that the inoculating dose did not affect the chronic-phase viremic set point (Fig. 3D). Durable SPgV infection could not be established in one macaque (cy0649) despite re-inoculation with $1.1 \times 10^7$ gc of SPgVkob from animal cy0575 at 43 dpi. Additionally, SPgV in plasma declined to undetectable levels after about 100 days of detectable viremia in four macaques, including the original two animals inoculated with olive baboon plasma, highlighting individual differences in the course of SPgV infection (Fig. 2).

### Baboon SPgVs elicit little to no disease in macaques

At no point after SPgV infection did macaques develop overt signs of disease, nor were gross hematologic or postmortem abnormalities observed in SIV-negative macaques infected with SPgV (fig. S2A). In 9 of 12 animals chronically infected with SIV and SPgV, liver sections revealed minimal to mild periportal and random lymphocytic hepatitis (fig. S2, B and C). The severity of hepatitis in these animals was not greater than typically noted in SIV-infected cynomolgus macaques.

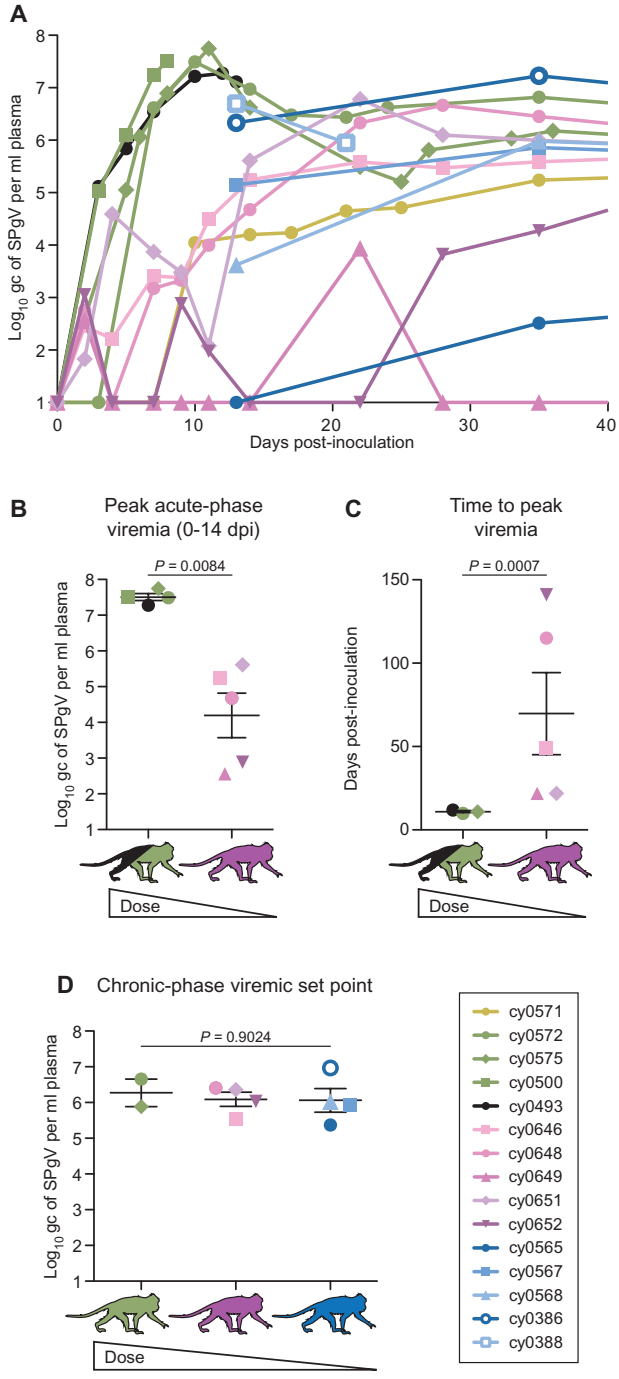


**Fig. 3. Inoculating dose affects acute-phase, but not chronic-phase, SPgV viremia.** (**A**) First 40 days of infection for all animals in this study. Graph highlights the predictable course of SPgVkob viremia in macaques inoculated with a high dose of SPgV and the highly variable course of SPgV viremia in macaques inoculated with a low dose of SPgVkob. (**B** and **C**) Quantification of peak viremia and time-to-peak viremia in high-dose versus low-dose groups (two-tailed unpaired *t* test; error bars represent SEM). (**D**) Comparison of set-point viremia, as defined by the average of at least three viral load measurements, taken over a period of at least 25 days, which did not differ by more than 1 $\log_{10}$ among groups receiving different doses of SPgVkob. One-way analysis of variance (ANOVA); error bars represent SEM.

### SPgVs exhibit a high degree of sequence stability

We performed deep sequencing of SPgVkob from several infected macaques at multiple time points (Fig. 2 and tables S3 to S5). Nucleotide variants that rose to greater than 50% of the within-host viral population were rare, with each intrahost viral population accumulating an average of 1.5 consensus-level variants per 100 days of infection, although no consensus-level variants were detected in some individuals despite persistent viremia (Fig. 4, A to C). Of the 11 nonsynonymous variants that were detected across all animals, 7 were due to one of two identical changes observed in the putative NS2 protein (Fig. 4, A, B, and D). One of these variants (T746M) was present at 0.72% in the inoculum administered to cy0565, cy0567, and cy0568 but was not detectable in the inoculum administered to cy0651 or cy0562, yet rose to near fixation in these five animals (Fig. 4D). A different amino acid substitution (A→V) was found at the same codon position in SPgVmyb at 219 dpi of cy0571 (table S5).

Sequencing analysis of SPgVmyb in wild yellow baboons revealed a degree of sequence stability similar to what we observed for SPgV in macaques, with *dN*/*dS* greater than 2.0 at only four sites throughout the genome (fig. S3). Subconsensus-level variation in SPgV-infected macaques was also low, with longitudinal intrahost analyses revealing a viral population that remained highly homogeneous during the acute-phase burst of viral replication and remained stable with low diversity throughout the chronic phase of infection (Fig. 5).

### SPgV is primarily bone marrow–tropic

Studies investigating the tissue tropism of HPgV have been limited (*19*–*21*). Therefore, we sought to comprehensively and quantitatively define the tissue distribution of SPgV at each stage of infection. We collected a large panel of tissues from four macaques (cy0500, cy0493, cy0388, and cy0571) at 8, 13, 21, and 219 dpi, respectively. RNA was extracted from each tissue sample, quantified by RT-qPCR, and normalized to obtain a tissue-specific viral load per milligram of tissue. To identify tissues containing SPgV RNA at concentrations greater than plasma, tissue viral loads were normalized to the plasma viral load (in microliters) of the respective individual at the time of tissue collection. This approach revealed that SPgV RNA is highly concentrated in only two tissues: the spleen and bone marrow (Fig. 6A). To investigate the relative contribution of each of these tissue compartments to systemic SPgV viral load (that is, virus production), we surgically removed the spleen from six macaques via laparotomy (that is, splenectomy) and closely monitored plasma viral loads for an extended period of time after splenectomy (Fig. 6B). With the exception of one macaque (cy0572), splenectomy did not have a significant effect on plasma viral load (Fig. 6, B and C).

To assess the concentration of SPgV RNA on a per-cell basis, we performed SPgV-specific RT-qPCR on leukocytes purified from spleen

**A**

| Animal ID | dpi | Position | Reference | Variant | Putative protein | AA change |
|---|---|---|---|---|---|---|
| cy0500 | 8 | — | — | — | — | — |
| cy0575 | 35 | — | — | — | — | — |
| cy0568 | 62 | 2664 | C | T | NS2 | **T746M** |
| cy0572 | 81 | 1477 | C | T | E2 | *Synonymous* |
| | | 1975 | A | G | E2 | *Synonymous* |
| cy0386 | 112 | — | — | — | — | — |
| cy0567 | 148 | 2664 | C | T | NS2 | **T746M** |
| | | 8851 | G | A | NS5B | *Synonymous* |
| cy0565 | 153 | 2664 | C | T | NS2 | **T746M** |
| cy0648 | 163 | 2411 | G | A | NS2 | **V662I** |
| cy0651 | 163 | 471 | — | A | Partial core protein | A15fs |
| | | 479 | T | — | E1 | S18fs |
| | | 1057 | G | A | E2 | *Synonymous* |
| | | 2411 | G | A | NS2 | **V662I** |
| | | 2664 | C | T | NS2 | **T746M** |
| | | 7015 | G | T | NS5A | *Synonymous* |
| cy0652 | 227 | 2056 | G | A | E2 | *Synonymous* |
| | | 2406 | C | T | NS2 | A660V |
| | | 2664 | C | T | NS2 | **T746M** |
| | | 6812 | T | C | NS5A | W2129R |
| | | 7051 | G | A | NS5A | *Synonymous* |

Total viremia days: 1152

**B**

| | Synonymous | Nonsynonymous | Total |
|---|---|---|---|
| Total variants | 7 | 11 | 18 |
| Total unique sites of variation | 7 | 6 | 12 |
| Average variants per animal | 0.78 | 1.22 | 2.00 |
| Average variants per 100 infection days | 0.61 | 0.95 | 1.56 |

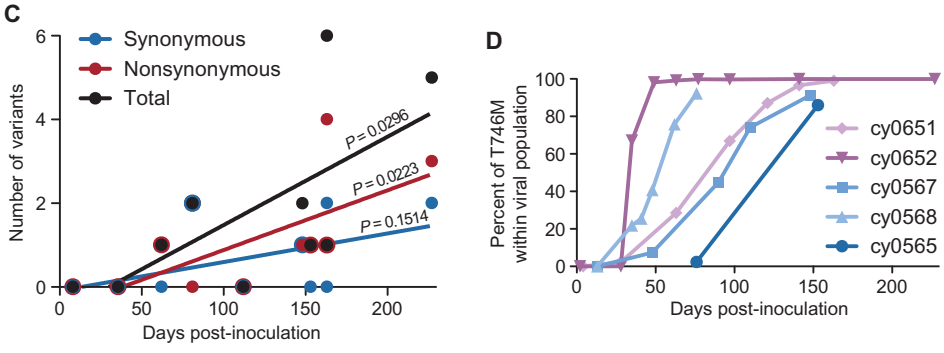


**Fig. 4. SPgV shows little nucleotide variation over the course of infection.** Deep sequencing reads from the latest available time point from each SPgVkob-infected animal were mapped to the SPgVkob_K23 reference genome (see tables S3 to S5 for sequencing statistics and details). (**A** to **C**) Consensus-level variants are shown for (A) each animal, (B) in summary, and (C) graphically. Univariate linear regression analysis with trend lines for synonymous (blue), nonsynonymous (red), and total variants (black). (**D**) Intrahost frequency of the most common mutation (T746M) over time in five macaques.

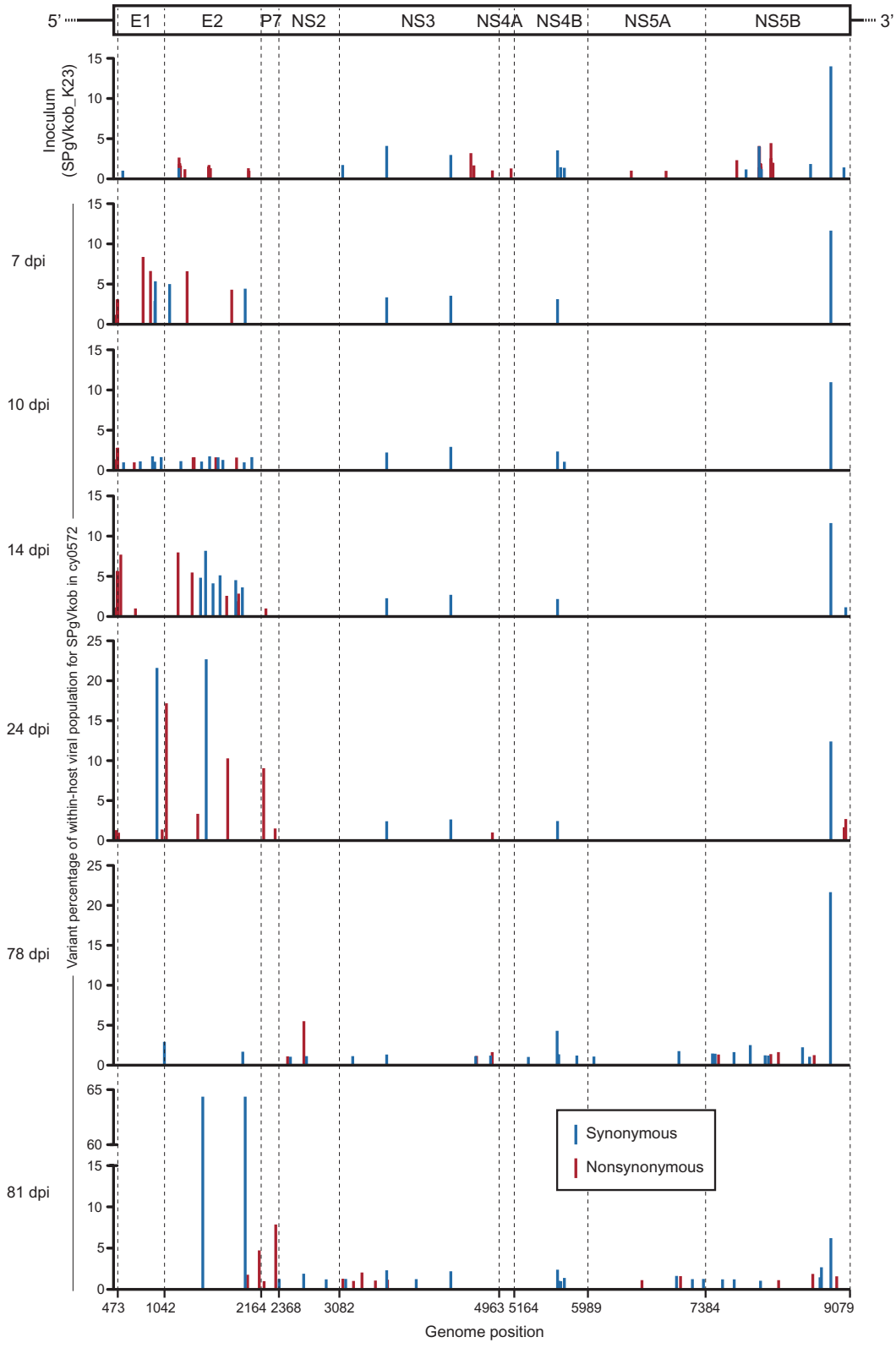


**Fig. 5. SPgV maintains low intrahost diversity over the course of infection.** Deep sequencing reads from time points throughout the infection of cy0572 were mapped to the SPgVkob_K23 reference genome, and variants >1% were identified (see table S4 for sequencing statistics and coverage details). A schematic of the SPgVkob genome with putative protein products is shown at the top. Blue bars represent synonymous variants present in the viral population, and red bars represent nonsynonymous variants.

and bone marrow. This approach also allowed us to measure SPgV viral loads in peripheral blood mononuclear cells (PBMCs), a lymphoid compartment in which HPgV RNA has been detected (*22*–*24*). No significant differences in the quantity of cell-associated SPgV RNA were observed between spleen, bone marrow, and PBMCs (Fig. 6D). However, stratification of these data by the phase of infection during which tissues were harvested suggests that RNA may be most concentrated in PBMCs during the acute phase and most concentrated in bone marrow during the chronic phase (fig. S4).

## DISCUSSION

HPgV infection is highly prevalent among humans, yet fundamental aspects of HPgV biology remain poorly understood. Our discovery of prevalent SPgV infection in yellow baboons from Tanzania extends the known host range and geographic range of these viruses and suggests that species-specific variants of SPgV maybe be widespread among primates. Infection of macaques—a "non-natural" host for these baboon SPgVs—did not elicit any overt signs of disease including histologic evidence of hepatitis during acute infection. In a fraction of animals evaluated in the chronic phase of SPgV infection, we observed histologic changes indicative of minimal to mild hepatitis. Although it seems likely that concurrent SIV infection contributed to the development of hepatitis in these animals, the severity of hepatitis we observed was still significantly less than reported previously in macaques inoculated with HPgV (*11*). The apparent nonpathogenicity of SPgVs from African Old World monkeys in macaques contrasts starkly with other blood-borne RNA viruses naturally found in African Old World monkeys, namely, the SIVs and simian arteriviruses (also known as simian hemorrhagic fever viruses), which respectively cause AIDS-like disease and viral hemorrhagic fever in macaques (*10*, *25*). This raises the intriguing possibility that PgV infection in primates may be universally nonpathogenic, although detailed long-term studies are needed to further examine PgV pathogenesis (or lack thereof).

This study provided the opportunity to examine the replication kinetics of SPgV during the acute phase of infection. We found that the acute phase of SPgV viremia was highly dependent on the infecting dose, with high-dose infections ($1.2 \times 10^7$ gc to $2.3 \times 10^7$ gc) reproducibly achieving a high-titer peak of viremia within the first 8 to 12 dpi, whereas low-dose infections ($6.4 \times 10^3$ gc to $6.0 \times 10^4$ gc) had a highly variable acute-phase viral load trajectory, with several animals not reaching their lifelong maximum of viremia until after 100 dpi. The high-titer viremia we observed within 2 weeks of SPgVkob inoculation in macaques is consistent with the kinetics of viremia seen in patients infected with HPgV via blood transfusion (*26*) but contrasts with experimental high-dose inoculation of HPgV in chimpanzees in which viremia was not detectable until 10 weeks after inoculation (*13*), possibly suggesting that the species barriers to PgV replication may be lower in baboons and macaques than in humans and chimpanzees. Additionally, the relationship between

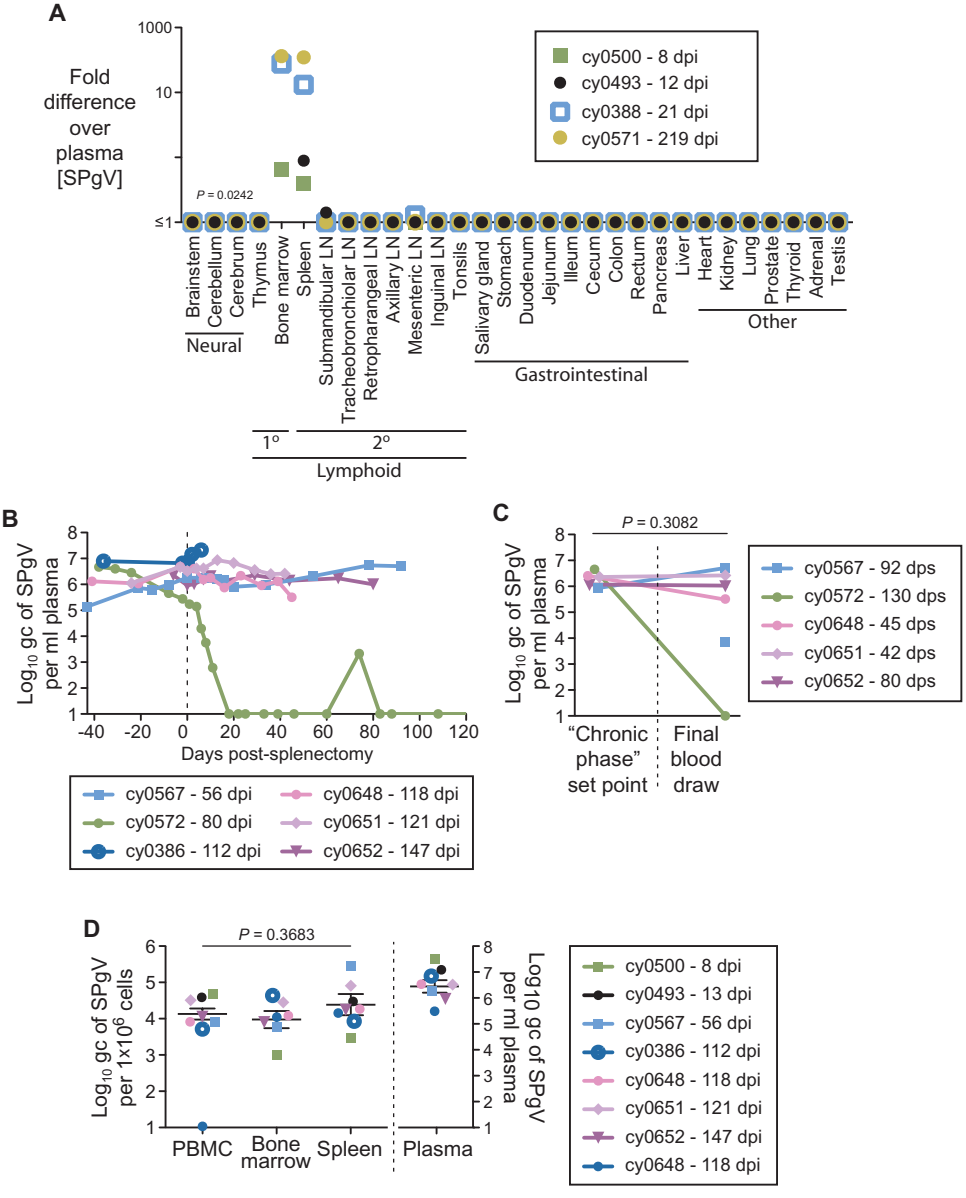


**Fig. 6. SPgV is primarily a bone marrow–tropic virus.** (**A**) Tissue viral load (gc/mg) normalized to plasma viral load (gc/μl), one-way ANOVA. Note that bone marrow was not recoverable from cy0493 due to atrophy. (**B** and **C**) Plasma viral loads before and after splenectomy, two-tailed paired *t* test. (**D**) Cell-associated viral loads (gc/1 × $10^6$ cells) performed in duplicate on RNA extracted from 3 × $10^6$ leukocytes purified from each tissue. One-way ANOVA; error bars represent SEM.

infecting dose and viral load trajectory is in contrast to HIV and SIV, which reproducibly replicate to a high-titer peak during the first few weeks of infection independent of infecting dose (*27*, *28*). The apparent connection between dose and viral load trajectory could explain the wide range of HPgV viral loads observed cross-sectionally in HPgV-infected humans (*29*, *30*), because people exposed via sexual contact may be infected by a relatively low dose, whereas those exposed via the administration of HPgV-positive blood products may be infected with a much greater dose (*31*–*36*). The eventual clearance of SPgV viremia by a minority of macaques inoculated with both high and low doses further underscores the heterogeneity of SPgV infection and is consistent with HPgV infection, as some humans eventually clear viremia, whereas others remain viremic indefinitely (*37*). The interplay between infecting dose, viral load trajectory, persistence, host genetics, and HPgV-mediated protection from HIV pathogenesis warrants further investigation.

Here, we examined SPgV sequence evolution in unprecedented detail. We observed remarkably little sequence evolution over hundreds of infection-days, with the virus maintaining strikingly low levels of intrahost nucleotide diversity and acquiring few to no consensus-level mutations despite high viremia. This is in contrast to other RNA viruses that cause persistent high-titer viremia (for example, HIV/SIV, hepatitis C virus, and simian arteriviruses), which exist as a genetically diverse swarm within infected hosts and accumulate variants in vivo at a rate that is orders of magnitude greater than what we observed for SPgV. Cellular and humoral immune responses are potent drivers of variant selection for these viruses, suggesting that SPgVs use a novel mechanism of persistence in which escape from host adaptive immune responses is largely unnecessary (*38*).

Of the six unique sites at which we observed nonsynonymous variation in SPgVkob, two sites had nonsynonymous changes in multiple macaques, and both of these sites were located within the putative NS2 protein. Remarkably, a nonsynonymous change was also observed in SPgVmyb in cy0571 at one of these sites. Although the role of NS2 in the pegivirus life cycle is still unclear, the rapid fixation of this NS2 variant in multiple animals infected with different viruses is indicative of a strong selective pressure at this particular site. Variation at this site is not observed among SPgV sequences from wild yellow baboons, red colobus monkeys, or red-tailed guenons, suggesting that this may be a macaque-specific adaptive change. However, fixation of this variant did not noticeably affect viral load or correlate with persistence/clearance.

Investigation of the tissue tropism of HPgV in vivo has been limited to tissues collected from a small number of HPgV-positive cadavers, evaluated for HPgV replication by negative strand–specific RT-PCR. This technique is highly influenced by the concentration of both viral positive-sense RNA and total RNA, which can result in self-priming (and/or false-priming) and a subsequent high rate of false-positive signals (*39*–*41*). Despite these limitations, two studies consistently detected HPgV negative-strand RNA in only two tissues: bone marrow and spleen, suggesting that these tissues are major sites of HPgV replication (*19*–*21*). Our study of SPgV tropism in macaques examined far more tissues using a concentration-based approach but ultimately gave a similar result, showing that SPgV RNA is concentrated in only the spleen and bone marrow of infected macaques. However, our data go further to suggest that viral replication in the spleen contributes minimally to viremia, because we observed no change in plasma viral titers after surgical removal of the spleen from several macaques. This suggests that bone marrow may be the primary site of SPgV replication. However, considering that we observed robust acute-phase SPgV replication in a macaque with very little active bone marrow (cy0493), it seems likely that SPgV production can occur in other tissues. One possible explanation for this observation may be that SPgV tropism shifts throughout infection, with the PBMCs and spleen supporting most of the viral replication early during infection and the bone marrow sustaining chronic, persistent infection.

The robust replication of baboon SPgVs in macaques appears to recapitulate key features of HPgV infection and is an advance for HPgV research. However, this study has several limitations. Most notably, the macaques infected with SPgV in this study were heterogeneous in several important respects including SIV status, SIV disease progression, age, sex, infecting SPgV strain, and infecting SPgV dose. Future studies that control for these factors are necessary to more clearly define the impact of these variables on SPgV infection. Controlling for variability in SIV pathogenesis will be particularly challenging but will be essential for the study of SPgV/SIV co-infection as a model of HPgV-mediated protection from HIV pathogenesis. Additional studies are also needed to determine whether our observations regarding SPgV tissue tropism and the effect of SPgV infecting dose on acute-phase viremia faithfully recapitulate HPgV infection in humans.

The cross-species transmission of an RNA virus that replicates to high titers and persists without accumulating genetic variation or causing disease violates conventional wisdom and could have far-reaching implications for understanding the interplay between viral persistence, inflammation, immune tolerance, and disease. Future studies should focus on identifying the cell types permissive for PgV replication and the mechanisms by which PgVs maintain persistence. Studies of macaques co-infected with SPgV and pathogenic SIV should also be prioritized, because this could shed light on the significant but poorly understood phenomenon of HPgV-mediated protection from immune activation and AIDS.

## MATERIALS AND METHODS

### Study design

This was a proof-of-concept study designed to establish a macaque model of HPgV infection. All protocols were approved by the University of Wisconsin–Madison Institutional Animal Care and Use Committee conforming to National Institutes of Health (NIH) animal care guidelines. A total of 14 macaques were infected with SPgVkob from an olive baboon ($1.2 \times 10^7$ gc to $2.3 \times 10^7$ gc, $n = 4$; $6.0 \times 10^4$ gc, $n = 5$; $6.4 \times 10^3$ gc, $n = 5$) and used to study viral transmission, tissue tropism, persistence, and intrahost evolution. One macaque was infected with $2.0 \times 10^5$ gc of SPgVmyb from two yellow baboons.

### Collection of samples from wild baboons

Blood samples from Kibale olive baboons (*P. anubis*) were collected in 2010 to 2014 as described previously (*15*, *42*), and approved by the Uganda Wildlife Authority (permit UWA/TDO/33/02), the Uganda National Council for Science and Technology (permit HS 364), and the University of Wisconsin Animal Care and Use Committee (protocol V01409-0-02-09). Samples were imported under CITES permit #002290 (Uganda). Samples from Mikumi yellow baboons (*P. cynocephalus*) were collected by Rogers and colleagues in 1985 and 1986 using standard methods for field studies of baboons as described previously (*43*). All procedures were approved by the appropriate Tanzanian government

authorities and by the U.S. institutions involved (Washington University and Yale University). Briefly, most study subjects were humanely trapped and sedated with ketamine. Blood samples were drawn from the femoral vein into evacuated blood collection tubes coated with EDTA anticoagulant. Animals were released as soon as possible after recovery from sedation. A small proportion of study subjects were sedated using a blowgun. These animals had blood collected in the same manner and were returned to their social group immediately after processing.

### Care and use of macaques at the Wisconsin National Primate Research Center

All macaque monkeys used in this study were cared for by the staff at the Wisconsin National Primate Research Center (WNPRC) in accordance with the regulations and guidelines outlined in the Animal Welfare Act and the *Guide for the Care and Use of Laboratory Animals*. Details of this study (University of Wisconsin–Madison Animal Care and Use Protocol No. G00707) were approved by the University of Wisconsin Institutional Animal Care and Use Committee, in accordance with recommendations of the Weatherall report. Animals used in this study were repurposed from several different studies, the details of which can be found in table S1.

**Inoculations.** Plasma samples were thawed at room temperature, and the appropriate volume (200 to 500 μl) was loaded into a 1-ml syringe and kept on ice until administration. Animals were sedated, and inocula were administered via an intravenous catheter followed by a sterile saline flush. At the conclusion of the procedure, anesthesia was reversed and animals were closely monitored by veterinary staff for adverse reactions and signs of disease.

**Deep sequencing.** Samples were processed for sequencing in a biosafety level 3 laboratory as described previously (*15*, *42*) with slight modifications. Briefly, for each animal, viral RNA was isolated from about 200 μl of plasma using the QIAamp MinElute virus spin kit (Qiagen), omitting carrier RNA. Samples were then treated with deoxyribonuclease (DNase), and complementary DNA (cDNA) synthesis was primed using random hexamers (Double-Stranded cDNA Synthesis Kit, Invitrogen). Samples were fragmented and sequencing adaptors were added using the Nextera DNA Sample Preparation Kit (Illumina). Deep sequencing was performed on the Illumina MiSeq. Sequence data were analyzed using CLC Genomics Workbench 6.5 (CLC bio) and Geneious R5 (Biomatters). Low quality (<Q30, Phred quality score) and short reads [<100 base pairs (bp)] were removed, and coding-complete (*44*) genome sequences for each virus were acquired using the de novo assembly algorithm in CLC Genomics Workbench version 6.5. Viral genomes were annotated in CLC Genomics Workbench version 6.5, and putative open reading frames were confirmed by querying the National Center for Biotechnology Information (NCBI) GenBank database (*45*).

**Phylogenetic analysis.** Complete coding sequences representing the known diversity of pegiviruses were aligned using a codon-based version of open source software multiple alignment using fast Fourier transform (MAFFT) (*46*) and cleaned using Gblocks, implemented in TranslatorX (*47*). Phylogenetic history was inferred from aligned nucleotide sequences using the maximum likelihood method (1000 bootstrap replicates) via Molecular Evolutionary Genetics Analysis version 6 (MEGA6) open source software (*48*). The best nucleotide substitution model, general time reversible model coupled with a Γ distribution for rate variation (GTR+Γ), was estimated using MEGA6. All positions containing gaps and missing data were eliminated, resulting in a final data set of 8118 positions. The initial tree for the heuristic search was obtained by applying the neighbor-joining method to a matrix of pairwise distances, estimated using the maximum composite likelihood approach.

**Evolutionary analysis.** Complete coding sequences for all 14 SPgVmyb genomes were aligned in CLC Genomics Workbench version 6.5. *dN* and *dS* were calculated using the HIV Synonymous Nonsynonymous Analysis Program (SNAP) version 2.1.1 (*49*, *50*) found at www.hiv.lanl.gov.

### Quantitative reverse transcription PCR

A TaqMan RT-qPCR assay was developed to quantify viral RNA for both SPgVkob (forward primer: 5′-CGGTGTTCATGGCAGGTAT-3′; reverse primer: 5′-CAGTTACAGCCGCGTGTTT-3′; probe: 5′-6FAM-ATGCACCCTGATGTAAGCTGGGCAA-BHQ1-3′) and SPgVmyb (forward primer: 5′-GGTTGGAGCCAGACTTAGCA-3′; reverse primer: 5′-CTAACACTTCCCGGCACATT-3′; probe: 5′-6FAM-CGGCTGTAACTGGCCTTTAC-BHQ1-3′). A standard curve was created by cloning a 381-bp fragment of the SPgVkob_K23 genome (forward primer: 5′-CCCCTCTGGTGTGGTTAGA-3′; reverse primer: 5′-CACTGATCGCCTCAGGTACA-3′) into the zero blunt PCR vector (Invitrogen), followed by linearization (Hind III, New England Biolabs) in vitro transcription for 6 hours (MEGAscript T7 Transcription Kit, Invitrogen), cleanup (MEGAclear Transcription Cleanup Kit, Invitrogen), quantification (Qubit RNA High-Sensitivity Assay Kit, Invitrogen), and dilution to a concentration of $1 \times 10^{10}$ transcript copies per microliter. Tenfold dilutions of this transcript were used as a standard curve for both SPgVkob and SPgVmyb. RNA was reverse-transcribed and amplified using the SuperScript III One-Step qRT-PCR system (Invitrogen) on a LightCycler 480 (Roche). Reverse transcription was carried out at 37°C for 15 min and then 50°C for 30 min followed by 2 min at 95°C, and then 50 cycles of amplification as follows: 95°C for 15 s and 60°C for 1 min. The reaction mixture contained $MgSO_4$ at a final concentration of 3.0 mM, with the two amplification primers at a concentration of 500 nM and probe at a concentration of 100 nM. The standard curve was linear over (at least) eight orders of magnitude and was sensitive down to 10 copies of RNA transcript per reaction.

**Purification of RNA from plasma.** Animals were sedated and blood was drawn from the femoral vein into an EDTA-treated vacutainer tube and centrifuged at 1400*g* for 7 min. Plasma was collected and centrifuged for an additional 5 min at 670*g* to remove residual cells. RNA was extracted from 300 μl of plasma using the Viral Total Nucleic Acid Purification Kit (Promega) on a Maxwell 16 MDx instrument.

**Purification of RNA from cells.** Macaques were appropriately sedated, and tissues were excised, chopped into ~1-cm cubes, and placed in 30 ml of ice-cold RPMI + 10% fetal calf serum (FCS) (Thermo Fisher Scientific). To achieve single-cell suspensions, tissues were manually disrupted with a scalpel and the butt of a sterile 60-ml syringe and then passed through a 100-μm cell strainer. Blood was overlayed on Ficoll at a 1:1 ratio and centrifuged at 1860*g* for 30 min to obtain PBMCs. Cells from each sample were washed with 40 ml of RPMI + 10% FCS, treated with ACK lysis buffer to remove red blood cells, and washed twice more with 40 ml of RPMI + 10% FCS. Centrifugations were performed at 670*g* for 5 min at 4°C, and samples were kept on ice throughout processing. Cells from each tissue were then counted (Z2 particle counter, Beckman Coulter). For each sample, $3.0 \times 10^6$ cells were disrupted using a QIAshredder column (Qiagen) and RNA was isolated using the Cells LEV Total RNA Purification Kit (Promega) on a Maxwell 16 MDx instrument. All extractions were performed in duplicate.

**Purification of RNA from tissues.** Immediately before euthanasia, macaques were sedated with ketamine and sodium pentobarbital was administered. Transcardiac perfusion of the entire body with 5 liters of sterile saline was performed to remove blood from the cardiovascular tree and vessels within tissues. Tissues were collected for routine histologic analysis, and three sections of each tissue (about 3 cm × 1 cm × 0.4 cm) were excised using autoclave-sterilized instruments and placed immediately into 12 ml of RNAlater (Sigma-Aldrich). Tissues were allowed to fix in RNAlater at 4°C overnight and then were removed, blotted, cut in sections weighing 20 to 50 mg, and stored in individual tubes at −80°C. Tissues were homogenized using the TissueLyser II (Qiagen) according to the manufacturer's instructions, and RNA was extracted from each tissue using the Tissue LEV Total RNA Purification Kit (Promega) on a Maxwell 16 MDx instrument.

**Splenectomy.** Animals were sedated and intubated. The spleen was surgically removed, and splenic vessels were ligated to prevent blood loss. At the conclusion of the procedure, animals were extubated and closely monitored by veterinary staff for adverse reactions and signs of disease.

### Statistical analysis

Phylogenetic analyses were performed using a maximum likelihood method (1000 bootstrap replicates) via MEGA6 open source software. Statistical analyses were performed using GraphPad Prism 5.0 software. Peak viremia and time-to-peak viremia in high-dose versus low-dose groups were compared using a two-tailed unpaired *t* test ($\alpha = 0.05$). Comparison of set-point viremia (as defined by the average of at least three viral load measurements taken over a period of at least 25 days that did not differ by more than 1 $\log_{10}$) among groups was performed using a one-way ANOVA ($\alpha = 0.05$). Synonymous and nonsynonymous mutation rates were analyzed using univariate linear regression. Viral loads from each tissue were compared using one-way ANOVA ($\alpha = 0.05$). Plasma viral loads before and after splenectomy were compared using a two-tailed paired *t* test ($\alpha = 0.05$). Viral loads from different cellular compartments were compared using one-way ANOVA.

## SUPPLEMENTARY MATERIALS

www.sciencetranslationalmedicine.org/cgi/content/full/7/305/305ra144/DC1
Fig. S1. Parameters of SIV-induced disease in study animals.
Fig. S2. Lack of SPgV-induced disease in study animals.
Fig. S3. SPgVs exhibit little sequence variability in natural hosts.
Fig. S4. The tissue tropism of SPgV may vary depending on the duration of infection.
Table S1. Sequencing of SPgVs from wild baboons.
Table S2. Demographic information for macaques used in this study.
Table S3. Sequencing of SPgVmyb in cy0571.
Table S4. Sequencing of macaques infected with SPgVkob.
Table S5. SPgVmyb consensus-level variants in cy0571 at 219 dpi not found in inocula.

## REFERENCES AND NOTES


1. N. Bhattarai, J. T. Stapleton, GB virus C: The good boy virus? *Trends Microbiol.* **20**, 124–130 (2012).
2. J. T. Stapleton, S. Foung, A. S. Muerhoff, J. Bukh, P. Simmonds, The GB viruses: A review and proposed classification of GBV-A, GBV-C (HGV), and GBV-D in genus *Pegivirus* within the family *Flaviviridae*. *J. Gen. Virol.* **92**, 233–246 (2011).
3. H. J. Alter, G-pers creepers, where'd you get those papers? A reassessment of the literature on the hepatitis G virus. *Transfusion* **37**, 569–572 (1997).
4. J. T. Stapleton, GB virus type C/hepatitis G virus. *Semin. Liver Dis.* **23**, 137–148 (2003).
5. M. D. Berzsenyi, D. J. Woollard, C. A. McLean, S. Preiss, V. M. Perreau, M. R. Beard, D. Scott Bowden, B. C. Cowie, S. Li, A. M. Mijch, S. K. Roberts, Down-regulation of intra-hepatic T-cell signaling associated with GB virus C in a HCV/HIV co-infected group with reduced liver disease. *J. Hepatol.* **55**, 536–544 (2011).
6. Y. Feng, L. Liu, Y. M. Feng, W. Zhao, Z. Li, A. M. Zhang, Y. Song, X. Xia, GB virus C infection in patients with HIV/hepatitis C virus coinfection: Improvement of the liver function in chronic hepatitis C. *Hepat. Mon.* **14**, e14169 (2014).
7. M. Lauck, A. L. Bailey, K. G. Andersen, T. L. Goldberg, P. C. Sabeti, D. H. O'Connor, GB virus C coinfections in West African Ebola patients. *J. Virol.* **89**, 2425–2429 (2015).
8. M. C. Lanteri, F. Vahidnia, S. Tan, J. T. Stapleton, P. J. Norris, J. Heitman, X. Deng, S. M. Keating, D. Brambilla, M. P. Busch, B. Custer; NHLBI REDS III Study, Downregulation of cytokines and chemokines by GB virus C after transmission via blood transfusion in HIV-positive blood recipients. *J. Infect. Dis.* **211**, 1585–1596 (2015).
9. W. Zhang, K. Chaloner, H. L. Tillmann, C. F. Williams, J. T. Stapleton, Effect of early and late GB virus C viraemia on survival of HIV-infected individuals: A meta-analysis. *HIV Med.* **7**, 173–180 (2006).
10. D. T. Evans, G. Silvestri, Nonhuman primate models in AIDS research. *Curr. Opin. HIV AIDS* **8**, 255–261 (2013).
11. H. Ren, F.-L. Zhu, M.-M. Cao, X.-Y. Wen, P. Zhao, Z.-T. Qi, Hepatitis G virus genomic RNA is pathogenic to Macaca mulatta. *World J. Gastroenterol.* **11**, 970–975 (2005).
12. Y. Cheng, W. Zhang, J. Li, B. Li, J. Zhao, R. Gao, S. Xin, P. Mao, Y. Cao, Serological and histological findings in infection and transmission of GBV-C/HGV to macaques. *J. Med. Virol.* **60**, 28–33 (2000).
13. J. Bukh, J. P. Kim, S. Govindarajan, C. L. Apgar, S. K. Foung, J. Wages, A. J. Yun, M. Shapiro, S. U. Emerson, R. H. Purcell, Experimental infection of chimpanzees with hepatitis G virus and genetic analysis of the virus. *J. Infect. Dis.* **177**, 855–862 (1998).
14. R. C. Jones, R. Greek, A review of the Institute of Medicine's analysis of using chimpanzees in biomedical research. *Sci. Eng. Ethics* **20**, 481–504 (2014).
15. S. D. Sibley, M. Lauck, A. L. Bailey, D. Hyeroba, A. Tumukunde, G. Weny, C. A. Chapman, D. H. O'Connor, T. L. Goldberg, T. C. Friedrich, Discovery and characterization of distinct simian pegiviruses in three wild African Old World monkey species. *PLOS One* **9**, e98569 (2014).
16. A. L. Bailey, M. Lauck, A. Weiler, S. D. Sibley, J. M. Dinis, Z. Bergman, C. W. Nelson, M. Correll, M. Gleicher, D. Hyeroba, A. Tumukunde, G. Weny, C. Chapman, J. H. Kuhn, A. L. Hughes, T. C. Friedrich, T. L. Goldberg, D. H. O'Connor, High genetic diversity and adaptive potential of two simian hemorrhagic fever viruses in a wild primate population. *PLOS One* **9**, e90714 (2014).
17. A. L. Bailey, M. Lauck, S. D. Sibley, J. Pecotte, K. Rice, G. Weny, A. Tumukunde, D. Hyeroba, J. Greene, M. Correll, M. Gleicher, T. C. Friedrich, P. B. Jahrling, J. H. Kuhn, T. L. Goldberg, J. Rogers, D. H. O'Connor, Two novel simian arteriviruses in captive and wild baboons (*Papio* spp.). *J. Virol.* **88**, 13231–13239 (2014).
18. M. Lauck, S. D. Sibley, D. Hyeroba, A. Tumukunde, G. Weny, C. A. Chapman, N. Ting, W. M. Switzer, J. H. Kuhn, T. C. Friedrich, D. H. O'Connor, T. L. Goldberg, Exceptional simian hemorrhagic fever virus diversity in a wild African primate community. *J. Virol.* **87**, 688–691 (2013).
19. T. Laskus, M. Radkowski, L. F. Wang, H. Vargas, J. Rakela, Detection of hepatitis G virus replication sites by using highly strand-specific Tth-based reverse transcriptase PCR. *J. Virol.* **72**, 3072–3075 (1998).
20. T. J. Tucker, H. E. Smuts, C. Eedes, G. D. Knobel, P. Eickhaus, S. C. Robson, R. E. Kirsch, Evidence that the GBV-C/hepatitis G virus is primarily a lymphotropic virus. *J. Med. Virol.* **61**, 52–58 (2000).
21. T. J. Tucker, H. E. Smuts, Review of the epidemiology, molecular characterization and tropism of the hepatitis G virus/GBV-C. *Clin. Lab.* **47**, 239–248 (2001).
22. S. L. George, J. Xiang, J. T. Stapleton, Clinical isolates of GB virus type C vary in their ability to persist and replicate in peripheral blood mononuclear cell cultures. *Virology* **316**, 191–201 (2003).
23. S. L. George, D. Varmaz, J. T. Stapleton, GB virus C replicates in primary T and B lymphocytes. *J. Infect. Dis.* **193**, 451–454 (2006).
24. E. T. Chivero, N. Bhattarai, R. T. Rydze, M. A. Winters, M. Holodniy, J. T. Stapleton, Human pegivirus RNA is found in multiple blood mononuclear cells in vivo and serum-derived viral RNA-containing particles are infectious in vitro. *J. Gen. Virol.* **95**, 1307–1319 (2014).
25. E. J. Snijder, M. Kikkert, Y. Fang, Arterivirus molecular biology and pathogenesis. *J. Gen. Virol.* **94**, 2141–2163 (2013).
26. H. J. Alter, Y. Nakatsuji, J. Melpolder, J. Wages, R. Wesley, J. W. Shih, J. P. Kim, The incidence of transfusion-associated hepatitis G virus infection and its relation to liver disease. *N. Engl. J. Med.* **336**, 747–754 (1997).
27. B. F. Keele, E. E. Giorgi, J. F. Salazar-Gonzalez, J. M. Decker, K. T. Pham, M. G. Salazar, C. Sun, T. Grayson, S. Wang, H. Li, X. Wei, C. Jiang, J. L. Kirchherr, F. Gao, J. A. Anderson, L.-H. Ping, R. Swanstrom, G. D. Tomaras, W. A. Blattner, P. A. Goepfert, J. M. Kilby, M. S. Saag, E. L. Delwart, M. P. Busch, M. S. Cohen, D. C. Montefiori, B. F. Haynes, B. Gaschen, G. S. Athreya, H. Y. Lee, N. Wood, C. Seoighe, A. S. Perelson, T. Bhattacharya, B. T. Korber, B. H. Hahn, G. M. Shaw, Identification and characterization of transmitted and early founder virus envelopes in primary HIV-1 infection. *Proc. Natl. Acad. Sci. U.S.A.* **105**, 7552–7557 (2008).

28. J. M. Greene, A. M. Weiler, M. R. Reynolds, B. T. Cain, N. H. Pham, A. J. Ericsen, E. J. Peterson, K. Crosno, K. Brunner, T. C. Friedrich, D. H. O'Connor, Rapid, repeated, low-dose challenges with SIVmac239 infect animals in a condensed challenge window. *Retrovirology* **11**, 66 (2014).
29. C. Li, P. Collini, K. Danso, S. Owusu-Ofori, A. Dompreh, D. Candotti, O. Opare-Sem, J. P. Allain, GB virus C and HIV-1 RNA load in single virus and co-infected West African individuals. *AIDS* **20**, 379–386 (2006).
30. M. T. Maidana-Giret, T. M. Silva, M. M. Sauer, H. Tomiyama, J. E. Levi, K. C. Bassichetto, A. Nishiya, R. S. Diaz, E. C. Sabino, R. Palacios, E. G. Kallas, GB virus type C infection modulates T-cell activation independently of HIV-1 viral load. *AIDS* **23**, 2277–2287 (2009).
31. V. R. Nerurkar, P. K. Chua, P. R. Hoffmann, W. M. Dashwood, C. M. Shikuma, R. Yanagihara, High prevalence of GB virus C/hepatitis G virus infection among homosexual men infected with human immunodeficiency virus type 1: Evidence for sexual transmission. *J. Med. Virol.* **56**, 123–127 (1998).
32. M. F. Scallan, D. Clutterbuck, L. M. Jarvis, G. R. Scott, P. Simmonds, Sexual transmission of GB virus C/hepatitis G virus. *J. Med. Virol.* **55**, 203–208 (1998).
33. G. Fiordalisi, A. Bettinardi, I. Zanella, R. Stellini, G. Paraninfo, G. Cadeo, D. Primi, Parenteral and sexual transmission of GB virus C and hepatitis C virus among human immunodeficiency virus-positive patients. *J. Infect. Dis.* **175**, 1025–1026 (1997).
34. J. J. Lefrere, F. Roudot-Thoraval, L. Morand-Joubert, Y. Brossard, F. Parnet-Mathieu, M. Mariotti, F. Agis, G. Rouet, J. Lerable, G. Lefevre, R. Girot, P. Loiseau, Prevalence of GB virus type C/hepatitis G virus RNA and of anti-E2 in individuals at high or low risk for blood-borne or sexually transmitted viruses: Evidence of sexual and parenteral transmission. *Transfusion* **39**, 83–94 (1999).
35. C. Seifried, M. Weber, H. Bialleck, E. Seifried, H. Schrezenmeier, W. K. Roth, High prevalence of GBV-C/HGV among relatives of GBV-C/HGV-positive blood donors in blood recipients and in patients with aplastic anemia. *Transfusion* **44**, 268–274 (2004).
36. P. Bjorkman, A. Naucler, N. Winqvist, I. Mushahwar, A. Widell, A case-control study of transmission routes for GB virus C/hepatitis G virus in Swedish blood donors lacking markers for hepatitis C virus infection. *Vox Sang.* **81**, 148–153 (2001).
37. J. J. Lefrère, P. Loiseau, J. Maury, J. Lasserre, M. Mariotti, N. Ravera, J. Lerable, G. Lefevre, L. Morand-Joubert, R. Girot, Natural history of GBV-C/hepatitis G virus infection through the follow-up of GBV-C/hepatitis G virus-infected blood donors and recipients studied by RNA polymerase chain reaction and anti-E2 serology. *Blood* **90**, 3776–3780 (1997).
38. J. T. Stapleton, J. Xiang, J. H. McLinden, N. Bhattarai, E. T. Chivero, D. Klinzman, T. M. Kaufman, Q. Chang, A novel T cell evasion mechanism in persistent RNA virus infection. *Trans. Am. Clin. Climatol. Assoc.* **125**, 14–24; discussion 24–26 (2014).
39. R. E. Lanford, C. Sureau, J. R. Jacob, R. White, T. R. Fuerst, Demonstration of in vitro infection of chimpanzee hepatocytes with hepatitis C virus using strand-specific RT/PCR. *Virology* **202**, 606–614 (1994).
40. T. Gunji, N. Kato, M. Hijikata, K. Hayashi, S. Saitoh, K. Shimotohno, Specific detection of positive and negative stranded hepatitis C viral RNA using chemical RNA modification. *Arch. Virol.* **134**, 293–302 (1994).
41. A. V. Timofeeva, N. A. Skrypina, Background activity of reverse transcriptases. *Biotechniques* **30**, 22–24 (2001).
42. M. Lauck, D. Hyeroba, A. Tumukunde, G. Weny, S. M. Lank, C. A. Chapman, D. H. O'Connor, T. C. Friedrich, T. L. Goldberg, Novel, divergent simian hemorrhagic fever viruses in a wild Ugandan red colobus monkey discovered using direct pyrosequencing. *PLOS One* **6**, e19056 (2011).
43. J. Rogers, thesis, Yale University (1989).
44. J. T. Ladner, B. Beitzel, P. S. Chain, M. G. Davenport, E. Donaldson, M. Frieman, J. Kugelman, J. H. Kuhn, J. O'Rear, P. C. Sabeti, D. E. Wentworth, M. R. Wiley, G. Y. Yu, S. Sozhamannan, C. Bradburne, G. Palacios, Standards for sequencing viral genomes in the era of high-throughput sequencing. *MBio* **5**, e01360-14 (2014).
45. S. F. Altschul, W. Gish, W. Miller, E. W. Myers, D. J. Lipman, Basic local alignment search tool. *J. Mol. Biol.* **215**, 403–410 (1990).
46. K. Katoh, K. Misawa, K. Kuma, T. Miyata, MAFFT: A novel method for rapid multiple sequence alignment based on fast Fourier transform. *Nucleic Acids Res.* **30**, 3059–3066 (2002).
47. F. Abascal, R. Zardoya, M. J. Telford, TranslatorX: Multiple alignment of nucleotide sequences guided by amino acid translations. *Nucleic Acids Res.* **38**, W7–W13 (2010).
48. K. Tamura, G. Stecher, D. Peterson, A. Filipski, S. Kumar, MEGA6: Molecular Evolutionary Genetics Analysis version 6.0. *Mol. Biol. Evol.* **30**, 2725–2729 (2013).
49. M. Nei, T. Gojobori, Simple methods for estimating the numbers of synonymous and nonsynonymous nucleotide substitutions. *Mol. Biol. Evol.* **3**, 418–426 (1986).
50. B. Korber, in *Computational Analysis of HIV Molecular Sequences*, A. G. Rodrigo, G. H. Learn, Eds. (Kluwer Academic Publishers, Dordecht, 2000), pp. 55–72.
51. P. Perelman, W. E. Johnson, C. Roos, H. N. Seuanez, J. E. Horvath, M. A. M. Moreira, B. Kessing, J. Pontius, M. Roelke, Y. Rumpler, M. P. C. Schneider, A. Silva, S. J. O'Brien, J. Pecon-Slattery, A molecular phylogeny of living primates. *PLOS Genet.* **7**, e1001342 (2011).



**Acknowledgments:** We thank the Department of Pathology and Laboratory Medicine (University of Wisconsin) and the WNPRC for funding and the use of its facilities and services. We thank W. Maury and J. Stapleton for helpful discussion. We thank J. Wada for artistic rendering of animal silhouettes. **Funding:** This work was funded by NIH grant TW009237 as part of the joint NIH–National Science Foundation Ecology of Infectious Diseases program and the UK Economic and Social Research Council, the Wisconsin Partnership Program through the Wisconsin Center for Infectious Diseases, and the NIH (R01 AI077376 and R01 AI084787). This publication was made possible in part by a grant (P51 RR000167) from the Office of Research Infrastructure Programs, a component of the NIH, to the WNPRC, University of Wisconsin–Madison. This research was conducted in part at a facility constructed with support from Research Facilities Improvement Program grants RR15459-01 and RR020141-01. A.L.B. performed this work with support from the University of Wisconsin's Medical Scientist Training Program (grant T32 GM008692) and a National Research Service Award through the Microbes in Health and Disease training program at the University of Wisconsin (T32 AI55397). Research reported in this publication was supported by the National Institute of General Medical Sciences of the NIH under Award Number T32GM081061. The content is solely the responsibility of the authors and does not necessarily represent the official views of the NIH. The funders of this research had no role in the study design, data collection and analysis, decision to publish, or preparation of the manuscript. **Author contributions:** A.L.B. and D.H.O. conceived the experimental design, with input from M.L., J.G., A.J.E., A.W., T.C.F., E.G.K., S.C., T.L.G., K.B., and H.A.S. A.L.B., M.L., and M.G. performed all sequencing. A.L.B. worked with M.M., J.M., A.W., G.L.-B., K.B., S.D.S., and H.A.S. to perform tissue and plasma viral load analyses. J.R. and T.L.G. provided plasma samples from wild baboons. E.J.P., K.B., K.G.B., K.C., A.M., S.C., and H.A.S. participated in animal care. A.L.B. wrote the manuscript. All authors edited and approved the manuscript. **Competing interests:** The authors declare that they have no competing interests. **Data and materials availability:** Coding-complete genome sequences for the SPgVmyb strains used in this study have been made available in GenBank under accession numbers KP890672-KP890673 and KR996142-KR996153. The coding-complete genome sequence for the SPgVkob strain used in this study was published previously (*15*) and can be found in the GenBank database under accession number KF234530.

Submitted 14 April 2015
Accepted 27 August 2015
Published 16 September 2015
10.1126/scitranslmed.aab3467

**Citation:** A. L. Bailey, M. Lauck, M. Mohns, E. J. Peterson, K. Beheler, K. G. Brunner, K. Crosno, A. Mejia, J. Mutschler, M. Gehrke, J. Greene, A. J. Ericsen, A. Weiler, G. Lehrer-Brey, T. C. Friedrich, S. D. Sibley, E. G. Kallas, S. Capuano III, J. Rogers, T. L. Goldberg, H. A. Simmons, D. H. O'Connor, Durable sequence stability and bone marrow tropism in a macaque model of human pegivirus infection. *Sci. Transl. Med.* **7**, 305ra144 (2015).

Science Translational Medicine

# Durable sequence stability and bone marrow tropism in a macaque model of human pegivirus infection

Adam L. Bailey, Michael Lauck, Mariel Mohns, Eric J. Peterson, Kerry Beheler, Kevin G. Brunner, Kristin Crosno, Andres Mejia, James Mutschler, Matthew Gehrke, Justin Greene, Adam J. Ericsen, Andrea Weiler, Gabrielle Lehrer-Brey, Thomas C. Friedrich, Samuel D. Sibley, Esper G. Kallas, Saverio Capuano III, Jeffrey Rogers, Tony L. Goldberg, Heather A. Simmons and David H. O'Connor

*Sci Transl Med* **7**, 305ra144305ra144.
DOI: 10.1126/scitranslmed.aab3467

**An animal model for the "Good Boy Virus"**

Human pegivirus (HPgV, formerly called GB virus C) can protect HIV-infected individuals from developing AIDS, a phenomenon that has earned it the nickname of the "Good Boy Virus." How HPgV imparts this protective effect remains a mystery, in part because no animal model of HPgV infection exists. Bailey and colleagues discovered viruses related to HPgV in wild baboons and showed that these viruses can infect laboratory macaque monkeys, providing unprecedented insights into the transmission, replication, and anatomical preference of HPgV with a view towards understanding HPgV-mediated protection from AIDS.



*Science Translational Medicine* (ISSN 1946-6242) is published by the American Association for the Advancement of Science, 1200 New York Avenue NW, Washington, DC 20005. The title *Science Translational Medicine* is a registered trademark of AAAS.